The Journal of Chemical Physics

Shape resonance determined from angular distribution in D_2 (v = 2, j = 2) + He → D_2 (v = 2, j = 0) + He cold scattering

Cite as: J. Chem. Phys. **154**, 104309 (2021); https://doi.org/10.1063/5.0045087
Submitted: 22 January 2021 . Accepted: 22 February 2021 . Published Online: 11 March 2021

Haowen Zhou, William E. Perreault, Nandini Mukherjee, and Richard N. Zare

COLLECTIONS

This paper was selected as an Editor's Pick

View Online Export Citation CrossMark

ARTICLES YOU MAY BE INTERESTED IN

Rainbow scattering in rotationally inelastic collisions of HCl and H_2
The Journal of Chemical Physics **154**, 104304 (2021); https://doi.org/10.1063/5.0043658

A dissipative particle dynamics model for studying dynamic phenomena in colloidal rod suspensions
The Journal of Chemical Physics **154**, 104120 (2021); https://doi.org/10.1063/5.0041285

Classical molecular dynamics
The Journal of Chemical Physics **154**, 100401 (2021); https://doi.org/10.1063/5.0045455

© 2021 Author(s).

The Journal of Chemical Physics ARTICLE scitation.org/journal/jcp

Shape resonance determined from angular distribution in D_2 (v = 2, j = 2) + He → D_2 (v = 2, j = 0) + He cold scattering

Cite as: J. Chem. Phys. 154, 104309 (2021); doi: 10.1063/5.0045087
Submitted: 22 January 2021 • Accepted: 22 February 2021 •
Published Online: 11 March 2021

View Online Export Citation CrossMark

Haowen Zhou, William E. Perreault, Nandini Mukherjee,[a] and Richard N. Zare[a]

AFFILIATIONS

Department of Chemistry, Stanford University, Stanford, California 94305, USA

[a]Authors to whom correspondence should be addressed: nmukherj@stanford.edu and zare@stanford.edu

ABSTRACT

We find an $l = 2$ shape resonance fingerprinted in the angular distribution of the cold (~1 K) $\Delta j = 2$ rotationally inelastic collision of D_2 with He in a single supersonic expansion. The Stark-induced adiabatic Raman passage is used to prepare D_2 in the (v = 2, j = 2) rovibrational level with control of the spatial distribution of the bond axis of the molecule by magnetic sublevel selection. We show that the rate of $\Delta j = 2$ D_2–D_2 relaxation is nearly two orders of magnitude weaker than that of D_2–He. This suggests that the strong D_2–He scattering is caused by an orbiting resonance that is highly sensitive to the shape of the long-range potential.

Published under license by AIP Publishing. https://doi.org/10.1063/5.0045087

INTRODUCTION

Low-energy gas-phase molecular collisions probe dynamic resonances that are formed within the centrifugal barrier of the colliding molecules.[1,2] These dynamic resonances represent collision complexes, which are positive energy quasi-bound states of the colliding pair that are highly sensitive to the structure of both short- and long-range interactions. The long-range portion of the interaction is of particular importance because of its role in initiating reactions at low collision energies. In search of scattering resonances, various molecular beam techniques have been employed to tune collision energies across a range from a few mK to a few Kelvin.[3–8] These experiments were highly successful in locating scattering resonances, but they were unable to provide a complete description of the dynamics because they did not measure the scattering angular distribution, which contains information on the contribution of each outgoing partial wave. In the presence of a scattering resonance, because only a select set of partial waves dominate, their interference generates a characteristic structure in the angular distribution. Indeed, recent low-energy collision experiments using velocity map imaging have begun to demonstrate some correlations between a scattering structure and its associated resonance.[9–11] However, these correlations are limited by the extent to which the internal states of the colliding molecules can be defined.

Recently, we conducted cold scattering experiments using quantum state-prepared HD (v = 1, j = 2) rotationally relaxing by collision with a ground state He atom.[12] The experimental scattering angular distributions showed a structure that correlated solely with a resonance associated with the $l = 2$ incoming partial wave. However, a later theoretical investigation found, instead, that the dominant resonance is from the l = 1 orbital.[13] Problematically, the theory did not show a satisfactory match with our experimentally measured angular distributions. Thus, the nature of this benchmark hydrogen–helium scattering resonance at low energies remains controversial. Additionally, the question of whether it is possible to establish a clear correlation between a measured scattering angular distribution and its associated resonance by precisely defining the quantum states needed to be verified by further experiments.

With this goal in mind, we studied the rotational relaxation of D_2 ($v = 2, j = 2$) → D_2 ($v = 2, j' = 0$) via collision with a ground state He atom in a co-expanded supersonic beam of D_2 and He. From the measured angular distributions, we are able to extract, without ambiguity, an l = 2 shape resonance. Earlier calculations[14] on the D_2–He collisions system do not show this resonance at the collision energies present here. To experimentally verify this resonance,

Published under license by AIP Publishing

we measured the same $\Delta j = 2$ rotational relaxation of D_2 ($v = 2$, $j = 2$) via another D_2 molecule in a pure D_2 molecular beam. Because the D_2–He system has nearly the same reduced mass as D_2–D_2, any difference in their scattering distribution must result from the difference in their scattering potentials. We measured the cross section for the D_2–D_2 collision to be nearly two orders of magnitude smaller than that of D_2–He. This experiment illustrates that a scattering resonance, which is highly sensitive to the long-range van der Waals interaction, is present for D_2–He and not for the D_2–D_2 collisions over the collision energy range studied. Our experimental investigation of the D_2–He rotationally inelastic cold collision shows that a scattering resonance is fingerprinted in the measured angular distribution when the quantum states of the reactants and products are fully controlled and selected.

EXPERIMENT AND ANALYSIS

Using the procedure extensively developed in our earlier work,[15] cold collisions were achieved by co-expanding a mixture of D_2 and He (ratio 1:10) using an Even–Lavie pulsed valve.[16] The adiabatically expanded gas is then collimated into a mixed molecular beam (divergence ≤ 12 mrad) using a skimmer. The co-expansion dramatically reduces the collision temperature (~1 K), while the collimated beam defines the direction of the collision velocity in the lab frame. Figure 1(a) shows the collision velocity distribution, which is calculated from the measured time-of-flight distribution of D_2 and He in the co-expanded beam.[15] From Fig. 1(a), we calculate a mean collision speed of 85 m/s and a mean collision temperature of 1.4 K. Figure 1(b) shows the orbital angular momentum $\sqrt{l(l+1)}$ as a function of the impact parameter b and the collision speed u for the incoming orbitals with $l = 1$, 2, 3, and 4. The black dashed line corresponds to the mean collision speed, and the gray dashed line corresponds to the limiting speed of 150 m/s, representing a range that includes 85% of the collisions. We only include impact parameters of up to 8 Å because prior theoretical work on the D_2–He van der Waals interaction[17] showed that the interaction potential falls to less than 10% of the average collision energy present in our experiment at this distance. For the collision velocity distribution of Fig. 1(a), it is clear that for $l = 1$ and 2, the impact parameter b falls within the 8 Å range of the D_2–He van der Waals interaction for a sizable fraction of the collisions. On the other hand, nearly all collisions for the $l = 3$ and 4 partial waves will have an impact parameter lying outside the interaction range. Thus, for the D_2–He collision speed distribution in Fig. 1(a), we can assume that only $l = 0$, 1, 2 contribute to the cold scattering. The rotational population distribution of D_2 ($v = 0$) in the D_2–He mixed beam was found to be ~55% in $j = 0$, ~32% in $j = 1$, ~10% in $j = 2$, and the rest ~3% in $j = 3$.

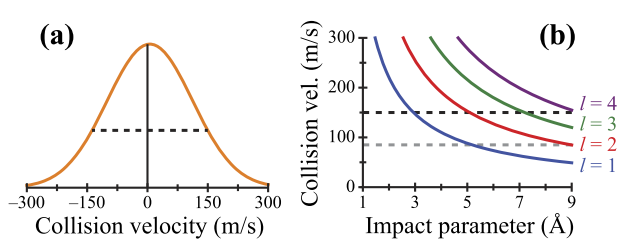

FIG. 1. Cold collisions in the mixed molecular beam restrict orbital angular momentum $l \leq 2$. (a) D_2–He collision velocity distribution (orange solid curve). The collision velocity distribution is calculated from individual D_2 and He Gaussian velocity distributions of the form $f(u) = \mathrm{Exp}\left[-((u-u_0)/\Delta)^2\right]$, where for He, $u_0 = 0$ and $\Delta = 121$ m/s and for D_2, $u_0 = -6$ m/s and $\Delta = 89$ m/s (see the supplementary material). The black dashed line indicates the range within which 85% of the collisions occurs. (b) Orbital angular momentum as a function of the collision speed and impact parameter. Solid curves represent $l = 1$ (blue), $l = 2$ (red), $l = 3$ (green), and $l = 4$ (purple). The black dashed line defines the range of 85% collisions. The gray dashed line refers to the mean collision speed of ~85 m/s.

A large fraction of the D_2 ($v = 0$, $j = 0$) population is pumped into the rovibrationally excited D_2 ($v = 2$, $j = 2$) state using the Stark-induced adiabatic Raman passage (SARP),[18–20] which employs two single-mode, partially overlapping nanosecond laser pulses to transfer population. Choosing the polarization of the SARP laser pulses allows for the control of the bond axis spatial distribution of the diatom by selecting specific m states within the rovibrational (v, j) eigenstate, where m represents the projection of the angular momentum vector j along a suitably chosen quantization z axis. To simplify the analysis, we choose the quantization axis along the collision velocity direction.[21] Using both laser polarizations aligned either parallel or perpendicular to the collision velocity direction, we prepare two specific bond axis alignments referred to as HSARP and VSARP. In HSARP, which prepares the pure state $|j = 2, m = 0\rangle$, the bond axis of D_2 ($v = 2$, $j = 2$) is preferentially aligned along the collision velocity, while for VSARP, which prepares the superposition state $-1/2|j = 2, m = 0\rangle + \sqrt{3/8}|j = 2, m = \pm 2\rangle$, the bond axis is aligned perpendicular to the collision velocity. Additionally, we use cross-polarized laser pulses to prepare the coherent superposition state $\sqrt{1/2}|j = 2, m = \pm 1\rangle$,[22] which we refer to as XSARP, where the bond axis is aligned at 45° relative to the collision velocity. The schematics in Fig. 2 show the three D_2 bond axis spatial distributions.[12,21,23]

The scattered D_2 ($v = 2$, $j' = 0$) molecules are state-selectively ionized using (2 + 1) REMPI at a delay of 400 ns following the SARP preparation of D_2 ($v = 2$, $j = 2$). The scattering angular distribution determined from the measured time-of-flight spectrum of the ions can be expressed for the HSARP, VSARP, and XSARP states as follows:

$$\left(\frac{d\sigma}{d\theta}\right)_H = \sin\theta \int_0^{2\pi} \left|q_{j=2,m=0\to j'=0}\right|^2 d\varphi, \tag{1}$$

$$\left(\frac{d\sigma}{d\theta}\right)_V = \sin\theta \int_0^{2\pi} \left| -\frac{1}{2} q_{j=2,m=0\to j'=0} + \sqrt{\frac{3}{8}}\left[q_{j=2,m=2\to j'=0} + q_{j=2,m=-2\to j'=0}\right]\right|^2 d\varphi, \tag{2}$$

and

$$\left(\frac{d\sigma}{d\theta}\right)_X = \sin\theta \int_0^{2\pi} \left|\sqrt{\frac{1}{2}} q_{j=2,m=1\to j'=0} + \sqrt{\frac{1}{2}} q_{j=2,m=-1\to j'=0}\right|^2 d\varphi. \tag{3}$$

Here, each $q_{j=2,\ m\to j'=0}$ in Eqs. (1)–(3) represents the probability amplitude to find the rotationally relaxed D_2 ($v = 2$, $j' = 0$) within the differential solid angle $d\Omega$ along (θ, φ). The angular distribution

Published under license by AIP Publishing

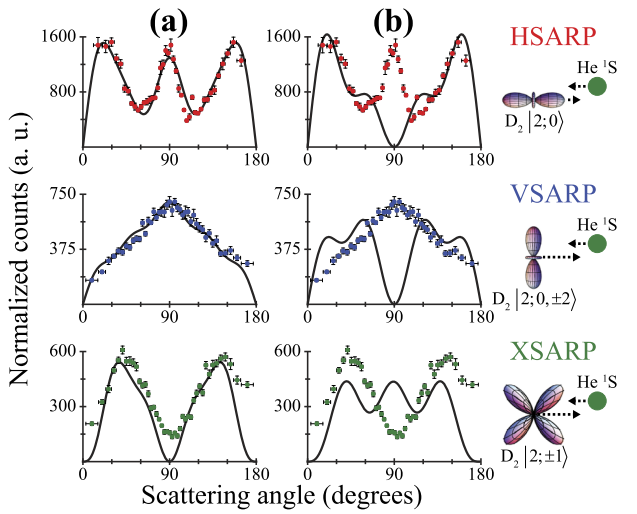

FIG. 2. Fitting of measured angular distributions with even and odd outgoing orbitals. Colored dots give experimental data, whereas black solid curves give the results of our partial wave analysis, as described in the text. The cartoons on the right show the collision geometry in the center-of-mass frame for each of the bond axis spatial distributions: HSARP, VSARP, and XSARP. (a) HSARP and VSARP fit ($R^2 > 0.99$) with the even outgoing orbitals $l' = 0, 2, 4$. For XSARP, the black curve is calculated ($R^2 = 0.94$) using the complex fitting coefficients found from HSARP and VSARP fits. (b) HSARP, VSARP, and XSARP fit with odd $l' = 1, 3$ outgoing orbitals following the same procedure. Clearly, we are not able to fit the experimental data using these partial waves.

results from the coherent superposition of the outgoing scattered orbitals, which can be expressed as follows:

$$q_{j=2,m\to j'=0} = \sum_{l',m_{l'}} c_{l'm_{l'}} Y_{l'm_{l'}}(\theta,\varphi). \tag{4}$$

In Eq. (4), $c_{l'm_{l'}}$ are the complex amplitudes for the outgoing orbital l'. The amplitudes $c_{l'm_{l'}}$ are proportional to the product of the scattering matrix elements $S^J(j = 2, l; j'l')$ and the Clebsch–Gordan coefficients describing coupling of the internal angular momentum j with the external orbital angular momentum l corresponding to the total angular momentum J that must be conserved in a collision. $S^J(j = 2, l; j'l')$ contains information about the dynamics of energy flow from the internal to the external degrees of freedom. Replacing $q_{j=2,m\to j'=0}$ in Eqs. (1)–(3) by the expansion given in Eq. (4), we obtain an integral expression for the scattering angular distribution. The complex amplitudes of the outgoing orbitals $(l', m_{l'})$ are then determined by numerically fitting the integral expression to the measured HSARP and VSARP angular distribution. Because the scattering matrix must be independent of the choice of the quantization axis, the fitting of the angular distributions is constrained by the relationships of the various $c_{l'm_{l'}}$ to $S^J(j = 2, l; j'l')$ that were described in detail in our earlier publication.[12]

In the following, we present a partial wave analysis of the angular distribution for the rotationally inelastic D_2 ($v = 2, j = 2$) → D_2 ($v = 2, j' = 0$) scattering. Our partial wave analysis is phenomenological and relies on the conservation of energy, momentum, angular momentum, and parity. A detailed description of our partial wave analysis can be found in our previous publications.[12,21,23] For the $\Delta j = 2$ collision, which results from quadrupolar interactions, the conservation of angular momentum and parity leads to the selection rule $\Delta l = 0, \pm 2$ for the orbital states. Thus, the scattering process preserves the parity of the incoming orbitals, so an even incoming orbital can only scatter into an even outgoing orbital. Additionally, the contributions of both positive and negative collision velocities must be included owing to the symmetric collision velocity distribution [see Fig. 1(a)].

We compare the fits of the HSARP and VSARP scattering angular distributions using either even, Fig. 2(a), or odd, Fig. 2(b), outgoing orbitals. In fitting the HSARP and VSARP distributions, a self-consistent set of complex coefficients or scattering matrix elements are obtained only for the even outgoing waves. Because the HSARP scattering is the simplest, involving only a single initial and a final state, we first determine the set of complex coefficients $c_{l'm_{l'}}$ that best fit the HSARP distribution. The VSARP distribution is then fit using only the one remaining unconstrained complex coefficient. These constrained fits with even outgoing partial waves give curves with $R^2 = 0.99$ for both the HSARP and VSARP distributions. The complex $S^J(jl; j'l')$ coefficients determined from the self-consistent fits are given in the supplementary material. Figure 2 also shows the XSARP scattering distribution, where the solid curve is not fit to the data but rather calculated using the determined values of $S^J(jl; j'l')$, giving an $R^2 = 0.94$. This further confirms the validity of the self-consistent $S^J(jl; j'l')$ coefficients extracted for the even outgoing orbitals $l' = 0, 2, 4$.

Following the procedure outlined above, we also attempt to fit the experimental data with the odd outgoing waves $l' = 1, 3$. Clearly, we are unable to find any reasonable fit with the angular distributions, as shown in Fig. 2(b). The obvious failure to find a consistent fit for the three alignments using the odd outgoing waves $l' = 1, 3$ suggests a minimal contribution from the $l = 1$ incoming orbital. Supporting this, we have also attempted to fit the angular distributions including both even and odd outgoing orbitals, but we found that the contribution of the odd orbitals was insignificant. These facts, together with the success of fitting with even orbitals, strongly indicate the presence of a scattering resonance that correlates with the incoming $l = 2$ orbital. Additionally, our measured scattering angular distributions for different alignments show striking similarity with previous theoretical calculations on an HD–He $l = 2$ resonance.[13]

To gain a deeper understanding of the scattering resonance, we studied the same rotational relaxation of D_2 ($v = 2, j = 2$) → D_2 ($v = 2, j' = 0$) via collision with another D_2 molecule in a supersonically expanded molecular beam of pure D_2. The rotational relaxation in a pure D_2 beam can be caused by collision either with another state-prepared D_2 ($v = 2, j = 2$) or by an unprepared D_2 in the ground vibrational level. The rotational population distribution of the ground D_2 ($v = 0$) vibrational level in a pure beam is measured to be ~38% in ($j = 0$), ~36% in ($j = 1$), ~24% in ($j = 2$), and ~2% in ($j = 3$). SARP transfers a large fraction of the D_2 ($v = 0, j = 0$) population to D_2 ($v = 2, j = 2$), and so, nearly all the available collision partners have $j > 0$. Because anisotropic forces are stronger for scattering partners with non-zero rotational angular momentum,[24] one might expect to see a significantly larger rate of $\Delta j = 2$ rotational relaxation of D_2 ($v = 2, j = 2$) in a pure beam compared to the D_2–He mixed beam. On the contrary, we found that the rate of rotational relaxation was reduced by nearly two orders of magnitude. The reduction

Published under license by AIP Publishing

TABLE I. Comparison of D_2–He and D_2–D_2 normalized scattering rates.

Alignment	Counts/hour in D_2–He mixed beam	Counts/hour in pure D_2 beam
HSARP	7000	30
VSARP	3700	120

was so substantial that we were unable to overcome the inherent experimental noise and generate a clean scattering angular distribution. Table I compares the rate of rotational relaxation of D_2 ($v = 2$, $j = 2$) in a mixed beam of He with that measured in the pure beam. For this comparison, we have appropriately normalized the scattered counts by the density of the colliding pairs in mixed and pure beams.

The D_2–He and D_2–D_2 collision complexes have nearly the same reduced mass, so the dramatic reduction in the scattering rate can only be explained by the difference in their long-range van der Waals interactions. This shows that the van der Waals interaction for the D_2–He scattering must support a quasi-bound D_2–He complex that strongly enhances the rate of collision. In the absence of this scattering resonance, the collision rate in the pure D_2 beam is severely reduced. A strong anisotropy in D_2–He scattering can be seen in Table I in that the HSARP rate is nearly twice that of VSARP. Moreover, we see that the preferred alignment for D_2–He is opposite to that for the D_2–D_2 scattering.

CONCLUSION

We showed here that the preparation of the internal state of D_2, coupled with a reduction in the collision temperature, allowed us to determine experimentally the dynamics of the D_2–He $\Delta j = 2$ rotationally inelastic collision. Our experiment illustrates that even with a relatively broad collision energy distribution, it is possible to detect a scattering resonance by its characteristic effect on the angular distribution. The strong, self-consistent fits of our experimental data shown here demonstrate the existence of a dominant $l = 2$ shape resonance for the low-energy hydrogen–helium collision system. A comparison to the $\Delta j = 2$ scattering in a pure D_2 beam, where the D_2–D_2 relaxation rate was dramatically reduced compared to D_2–He, strongly suggests that rotational relaxation is mediated by an orbiting resonance.

The dominance of a single $l = 2$ resonance is not intuitive, given the relatively broad velocity distribution shown in Fig. 1(a), which can support multiple resonances. In fact, $l = 1$ collisions are statistically most common for our energy spectrum. However, the complete failure to fit the angular distributions with odd outgoing orbitals $l' = 1, 3$ proves that the $l = 1$ input wave has negligible contribution to the scattering process. The small contribution from the $l = 1$ orbital might be explained by recalling that our experiments measure the collision rate, not the cross section. As such, the number of scattered counts is proportional to the collision speed: $N_C \propto \sigma_{j=2\to j'=0} \int uf(u)du$, where $\sigma_{j=2\to j'=0}$ is the cross section and $f(u)$ gives the collision speed distribution of Fig. 1(a). Using the calculated energy (~0.02 K)[14] for the $l = 1$ D_2–He collision resonance, we can estimate a rate factor $\int uf(u)du$ using our collision speed distribution of Fig. 1(a). Using the height of the centrifugal barrier, we estimated an upper limit for the resonance energy of the $l = 2$ orbital. The height of the barrier was calculated using the available H_2–He van der Waals potential[17] and the centrifugal energy $l(l+1)\hbar^2/2\mu r^2$. This gives the energy that corresponds to a classical orbiting resonance, but the actual tunneling resonance energy is expected to be slightly less than the barrier height. From this estimated upper limit, we find that the rate factor is roughly 10 times larger for $l = 2$ than for $l = 1$. This may explain the complete absence of $l = 1$ signature in our scattering angular distribution.

On the contrary, theoretical calculations[13,14] on this system show only a strong $l = 1$ resonance, with the $l = 2$ resonance either weak or completely absent. Disagreement between our experimental results and theoretical calculations might arise from the extreme sensitivity of resonance behavior to the long-range portion of the anisotropic potential that drives the $\Delta j = 2$ transition. This sensitivity was vividly demonstrated in a recent study on the Penning ionization of molecular hydrogen.[25] Crucially, the angular part of the anisotropic potential depends on the rotational wave function including its alignment. The preparation of the D_2 molecules in the ($v = 2$) vibrationally excited state is another possible explanation for the discrepancy because low-energy scattering resonances depend sensitively on the vibrational state.[26] These discrepancies are only beginning to come to light because of the unprecedented control over quantum states that we have recently achieved. Our experiments show that when the scattering process is completely controlled, the measured angular distribution contains a wealth of information about the dynamics of a scattering resonance. These experiments thus provide important insights directly into molecular interaction forces and additionally serve as a reference against which theoretical calculations can be directly compared.

SUPPLEMENTARY MATERIAL

See the supplementary material for the experimentally measured He and D_2 velocity distributions and the calculated collision temperature as well as the scattering matrix elements $S^l(jl; j'l')$ determined from the fit to the measured angular distributions.

ACKNOWLEDGMENTS

This work was supported by the U.S. Army Research Office under ARO Grant No. W911NF-19-1-0163 and MURI Grant No. W911NF-19-1-0283.

DATA AVAILABILITY

The data that support the findings of this study are available from the corresponding author upon reasonable request.

REFERENCES

[1] C. Naulin and M. Costes, "Experimental search for scattering resonances in near cold molecular collisions," Int. Rev. Phys. Chem. **33**, 427–446 (2014).
[2] M. Costes and C. Naulin, "Observation of quantum dynamical resonances in near cold inelastic collisions of astrophysical molecules," Chem. Sci. **7**, 2462–2469 (2016).
[3] A. B. Henson, S. Gersten, Y. Shagam, J. Narevicius, and E. Narevicius, "Observation of resonances in penning ionization reactions at sub-kelvin temperatures in merged beams," Science **338**, 234–239 (2012).

Published under license by AIP Publishing

[4]S. Chefdeville *et al.*, "Appearance of low energy resonances in CO-*para*-H_2 inelastic collisions," Phys. Rev. Lett. **109**, 023201 (2012).
[5]S. Chefdeville, Y. Kalugina, S. Y. T. van de Meerakker, C. Naulin, F. Lique, and M. Costes, "Observation of partial wave resonances in low-energy O_2-H_2 inelastic collisions," Science **341**, 1094–1096 (2013).
[6]B. Bertsche, J. Jankunas, and A. Osterwalder, "Low-temperature collisions between neutral molecules in merged molecular beams," CHIMIA Int. J. Chem. **68**, 256–259 (2014).
[7]A. Bergeat, J. Onvlee, C. Naulin, A. van der Avoird, and M. Costes, "Quantum dynamical resonances in low-energy CO(j = 0) + He inelastic collisions," Nat. Chem. **7**, 349–353 (2015).
[8]D. Bhattacharya, M. Pawlak, A. Ben-Asher, A. Landau, I. Haritan, E. Narevicius, and N. Moiseyev, "Quantum effects in cold molecular collisions from spatial polarization of electronic wave function," J. Phys. Chem. Lett. **10**, 855–863 (2019).
[9]S. N. Vogels, J. Onvlee, S. Chefdeville, A. van der Avoird, G. C. Groenenboom, and S. Y. T. van de Meerakker, "Imaging resonances in low-energy NO-He inelastic collisions," Science **350**, 787–790 (2015).
[10]S. N. Vogels, T. Karman, J. Kłos, M. Besemer, J. Onvlee, A. van der Avoird, G. C. Groenenboom, and S. Y. T. van de Meerakker, "Scattering resonances in bimolecular collisions between NO radicals and H_2 challenge the theoretical gold standard," Nat. Chem. **10**, 435 (2018).
[11]P. Paliwal, N. Deb, D. M. Reich, A. v. d. Avoird, C. P. Koch, and E. Narevicius, "Determining the nature of quantum resonances by probing elastic and reactive scattering in cold collisions," Nat. Chem. **13**, 94–98 (2021).
[12]W. E. Perreault, N. Mukherjee, and R. N. Zare, "HD (v = 1, j = 2, m) orientation controls HD-He rotationally inelastic scattering near 1 K," J. Chem. Phys. **150**, 174301 (2019).
[13]M. Morita and N. Balakrishnan, "Stereodynamics of rotationally inelastic scattering in cold He + HD collisions," J. Chem. Phys. **153**, 091101 (2020).
[14]B. Zhou and M. Chen, "Quantum rotational scattering of H_2 and its isotopologues with He," Mol. Phys. **115**, 2442–2450 (2017).
[15]W. E. Perreault, N. Mukherjee, and R. N. Zare, "Supersonic beams of mixed gases: A method for studying cold collisions," Chem. Phys. **514**, 150–153 (2018).
[16]U. Even, "The Even-Lavie valve as a source for high intensity supersonic beam," EPJ Tech. Instrum. **2**, 17 (2015).
[17]W. Meyer, P. C. Hariharan, and W. Kutzelnigg, "Refined ab initio calculation of the potential energy surface of the He-H_2 interaction with special emphasis to the region of the van der Waals minimum," J. Chem. Phys. **73**, 1880–1897 (1980).
[18]W. E. Perreault, N. Mukherjee, and R. N. Zare, "Stark-induced adiabatic Raman passage examined through the preparation of D_2 (v = 2, j = 0) and D_2 (v = 2, j = 2, m = 0)," J. Chem. Phys. **150**, 234201 (2019).
[19]W. E. Perreault, H. Zhou, N. Mukherjee, and R. N. Zare, "Harnessing the power of adiabatic curve crossing to populate the highly vibrationally excited H_2 (v = 7, j = 0) level," Phys. Rev. Lett. **124**, 163202 (2020).
[20]N. Mukherjee, W. E. Perreault, and R. N. Zare, "Stark-induced adiabatic passage processes to selectively prepare vibrationally excited single and superposition of quantum states," in *Frontiers and Advances in Molecular Spectroscopy* (Elsevier, Inc., 2018), pp. 1–46.
[21]W. E. Perreault, N. Mukherjee, and R. N. Zare, "Quantum control of molecular collisions at 1 Kelvin," Science **358**, 356–359 (2017).
[22]N. Mukherjee, W. Dong, and R. N. Zare, "Coherent superposition of M-states in a single rovibrational level of H_2 by Stark-induced adiabatic Raman passage," J. Chem. Phys. **140**, 074201 (2014).
[23]W. E. Perreault, N. Mukherjee, and R. N. Zare, "Quantum controlled rotationally inelastic scattering of HD with H_2 and D_2 near 1 Kelvin reveals collisional partner reorientation," Nat. Chem. **10**, 561–567 (2018).
[24]Y. Shagam, A. Klein, W. Skomorowski, R. Yun, V. Averbukh, C. P. Koch, and E. Narevicius, "Molecular hydrogen interacts more strongly when rotationally excited at low temperatures leading to faster reactions," Nat. Chem. **7**, 921–926 (2015).
[25]A. Klein, Y. Shagam, W. Skomorowski, P. S. Żuchowski, M. Pawlak, L. M. C. Janssen, N. Moiseyev, S. Y. T. van de Meerakker, A. van der Avoird, C. P. Koch, and E. Narevicius, "Directly probing anisotropy in atom-molecule collisions through quantum scattering resonances," Nat. Phys. **13**, 35–38 (2017).
[26]J. L. Nolte, P. C. Stancil, T.-G. Lee, N. Balakrishnan, and R. C. Forrey, "Rovibrational quenching rate coefficients of HD in collisions with He," Astrophys. J. **744**, 62 (2012).

Published under license by AIP Publishing